THE ASTROPHYSICAL JOURNAL, 238:471–487, 1980 June 1

ROTATIONAL PROPERTIES OF 21 Sc GALAXIES WITH A LARGE RANGE OF LUMINOSITIES AND RADII, FROM NGC 4605 ($R = 4$ kpc) TO UGC 2885 ($R = 122$ kpc)

VERA C. RUBIN,[1,2] W. KENT FORD, JR.,[1] AND NORBERT THONNARD
Department of Terrestrial Magnetism, Carnegie Institution of Washington
Received 1979 October 11; accepted 1979 November 29

ABSTRACT

For 21 Sc galaxies whose properties encompass a wide range of radii, masses, and luminosities, we have obtained major axis spectra extending to the faint outer regions, and have deduced rotation curves. The galaxies are of high inclination, so uncertainties in the angle of inclination to the line of sight and in the position angle of the major axis are minimized. Their radii range from 4 to 122 kpc ($H = 50$ km s^{-1} Mpc^{-1}); in general, the rotation curves extend to 83% of $R_{25}{}^{i,b}$. When plotted on a linear scale with no scaling, the rotation curves for the smallest galaxies fall upon the initial parts of the rotation curves for the larger galaxies. All curves show a fairly rapid velocity rise to $V \sim 125$ km s^{-1} at $R \sim 5$ kpc, and a slower rise thereafter. Most rotation curves are rising slowly even at the farthest measured point. Neither high nor low luminosity Sc galaxies have falling rotation curves. Sc galaxies of all luminosities must have significant mass located beyond the optical image. A linear relation between log V_{max} and log R follows from the shape of the common rotation curve for all Sc's, and the tendency of smaller galaxies, at any R, to have lower velocities than the large galaxies at that R. The significantly shallower slope discovered for this relation by Tully and Fisher is attributed to their use of galaxies of various Hubble types and the known correlation of V_{max} with Hubble type.

The galaxies with very large central velocity gradients tend to be large, of high luminosity, with massive, dense nuclei. Often their nuclear spectra show a strong stellar continuum in the red, with emission lines of [N II] stronger than Hα. These galaxies also tend to be 13 cm radio continuum sources.

Because of the form of the rotation curves, small galaxies undergo many short-period, very differential, rotations. Large galaxies undergo (in their outer parts) few, only slightly differential, rotations. This suggests a relation between morphology, rotational properties, and the van den Bergh luminosity classification, which is discussed. UGC 2885, the largest Sc in the sample, has undergone fewer than 10 rotations in its outer parts since the origin of the universe but has a regular two-armed spiral pattern and no significant velocity asymmetries. This observation puts constraints on models of galaxy formation and evolution.

Subject heading: galaxies: internal motions

I. INTRODUCTION

Several years ago, we embarked on an observational program to obtain the rotational properties of spiral galaxies to their faint outer limits, in an attempt to understand which dynamical properties are significant in determining the Hubble classification of a spiral galaxy. A few initial results from this study have already been published: a brief account of the dynamical properties of a set of high-luminosity spirals from Sa through Sc (Rubin, Ford, and Thonnard 1978, Paper IV), details of one Sc (Rubin, Thonnard, and Ford 1977*a*, Paper I), one Sb (Peterson *et al.* 1978, Paper III), and one Sa (Rubin *et al.* 1978, Paper II). In the present paper, we discuss the rotational properties of an extensive set of Sc galaxies with a wide range in luminosity. In later papers we will discuss the masses, the luminosities, and their relations to the dynamical properties of Sc galaxies (Rubin and Burstein 1980), and the interrelation between the dynamics and the morphologies of the sample galaxies (Kormendy and Rubin 1980).

Although Sc's exhibit extremely wide ranges of luminosities and masses, no systematic study of their rotational properties has previously been attempted. We present here the velocities for 21 Sc galaxies, with luminosities which range from 3×10^9 to 2×10^{11} $L_\odot$, masses from 10^{10} to 2×10^{12} $M_\odot$, and radii from 4 to 122 kpc. The galaxies were chosen with extreme care from the *Revised Shapley Ames*

[1] Visiting Astronomer, Kitt Peak National Observatory, which is operated by the Association of Universities for Research in Astronomy, Inc., under contract with the National Science Foundation.

[2] Visiting Astronomer, Cerro Tololo InterAmerican Observatory, supported by the National Science Foundation under contract No. AST 74-04128.

TABLE 1

PARAMETERS FOR PROGRAM Sc GALAXIES

NGC	Class RSA	V_o km/s	V_c km/s	Distance Mpc	Observed Position Angles	Ø (°)	i (°)	Radius (')	R_{25} kpc	Δm_b mag	$R^{i,b}$ kpc	$R_{farthest}$ kpc	$\frac{R_f}{R^{i,b}}$	V_{max} km/s
(1)	(2)	(3)	(4)	(5)	(6)	(7)	(8)	(9)	(10)	(11)	(12)	(13)	(14)	(15)
4605	Sc(s)III	150±25	288*	5.8	122, 110	110:D	68	2.75	4.60	0	4.29	3.3	0.77	101
1035	Sc:III	1230±10	1227*	24.5	138, 60	142D	71	1.12	8.00	0.02	7.46	7.0	0.94	128
4062	Sc(s)II-III	747±10	742*	14.8	104	104	64	2.14	9.22	0	8.80	9.0	1.02	163
2742	Sc(r)II	1267±10	1363*	27.3	88, 178	88D	58	1.55	12.3	0.18	12.5	10.6	0.85	171
701	Sc(s)II.2:	1795±10	1825*	36.5	43	43	61	1.26	13.4	0.02	12.7	7.7	0.61	151
2608	ScII:	2125±15	2059*	41.2	62	62	50	1.26	15.0	0.10	15.1	11.7	0.78	132
3495	Sc(s)III	1114±15	952*	19.0	20, 110	25D	78	2.29	12.6	0.79	15.2	12.7	0.84	179
1087	Sc(s)III.3	1503±10	1523*	30.5	1	1	50	1.74	15.3	0.10	15.4	11.0	0.71	140
U3691	(Sc)	2182±15	2076*	41.5	65	65	65	1.2	14.5	0.62	16.6	14.0	0.84	134
4682	Sc(s)II.4	2307±10	2152*	43.0	87	87	57	1.41	17.7	0.09	17.3	14.8	0.86	178
3672	Sc(s)I-II	1857±10	1655	33.1	8, 98	8D	70	2.03	19.5	0.06	18.7	17.8	0.95	192
1421	ScIII:	2063±15	1985*	39.7	1	1	78	1.82	21.0	0.09	19.5	20.0	1.03	208
2715	Sc(s)II	1308±10	1487*	29.7	20	20	70	2.51	21.7	0.01	20.2	18.4	0.91	160
4321	Sc(s)I	1545±25	1478*	20	110, 140, 35	155:D	35	3.46	20.1	0.03	20.1	14.6	0.73	210
IC467	(Sc)	2025±15	2213*	44.3	72	72	67	1.70	21.9	0.13	21.4	20.9	0.98	152
7541	ScIII:	2685±10	2873	57.5	79, 102	102	72	1.74	29.0	0.20	28.4	23.0	0.81	247
7664	(Sc)	3464±15	3709	74.2	90, 6	94D	58	1.65	35.6	0.16	34.9	28.0	0.80	203
2998	Sc(rs)I	4767±15	4781	95.6	53, 143	52D	62	1.51	42.0	0	40.0	34.0	0.85	215
753	Sc(rs)I	4895±25	5077*	101.5	125	125	50	1.44	42.4	0.21	44.6	24.7	0.55	221
801	(Sc)	5763±15	5948	119.	150, 49	150D	86	1.65	57.1	0.19	53.5	47.4	0.89	232
U2885	(Sc)	5785±25	5887*	118.	140, 40, 43	50D	65	2.75	94.2	1.04	122.	82.3	0.67	280

Notes: Column (1) U = Uppsala General Catalogue (Nilsson, 1973).
(2) Classification from RSA (Sandage and Tammann, 1980); those not in RSA (in parentheses) from UGC.
(4) $V + 300 \sin l \cos b$; * denotes night sky lines used as velocity standard.
(5) D = $V_c/50$ Mpc; except NGC 4321 D = 20 Mpc, adopted for Virgo cluster.
(7) ϕ adopted; D denotes ϕ determined dynamically from plates in 2 or more position angles.
(8) i from RC2, except NGC 3672 (Paper 1); NGC 4321 (van der Kruit, 1973); NGC 2608, 1087, and 753, $i = 50°$ adopted.
(9) Radius in arc min from RC2; to 25 mag arcsec^{-2}.
(10) R_{deV} in kpc calculated from D(25) in RC2 and adopted distance; for UGC galaxies log D(25) = 0.11 + 0.92 log D(UGC) as derived in RC2.
(11) Burstein and Heiles, 1979.
(12) log $R^{i,b}$ = log $R(25) \Rightarrow 0.07 \log a/b - \log (1 - A_b/3.35)$; (Burstein and Heiles, 1979).
(13) Radial distance of outermost measured velocity.

NOTES FOR INDIVIDUAL GALAXIES

NGC 4605.—Poorly defined irregular structure, poorly defined nucleus. Nuclear velocity gradient on sky $= +1.95$ km s^{-1} arcsec^{-1} in PA 110°, and $+1.68$ in PA 122°. (Here and in the following notes, nuclear velocity gradients are called positive if the velocity variation across the nucleus is positive in going N through E; it is called negative if the velocity variation is negative, N through E.) $\phi = 110°$ adopted; it may be smaller. Large velocity gradients ~ -25 km s^{-1} per 500 pc near edge of optical galaxy. [S II] more intense than [N II] throughout galaxy. NGC 4605 is a nearby field galaxy, within 10 Mpc (Kraan-Korteweg and Tammann 1979).

NGC 1035.—Knotty multiarmed structure. Nuclear velocity gradient $= -8.55$ km s^{-1} arcsec^{-1} in PA 138°, and -1.27 in PA 60°. [S II] $\leq$ [N II] λ6583.

NGC 4062.—Well defined nucleus; intermediate between two-armed global and multiarmed spiral. Nuclear emission discontinuous, steep nuclear velocity gradient. Emission strongest off nucleus; [S II] $\leq$ [N II] λ6583.

NGC 2742.—Well defined nucleus and multiarmed spiral. Steep nuclear velocity gradient; rotation curve only moderately symmetric.

NGC 701.—Poorly defined spiral structure; elongated nucleus (bar?). Steep nuclear velocity gradient; nuclear emission discontinuous. Power failures interrupted several exposures; only the 15^{m} exposure shown has been measured.

NGC 2608.—Intense stellar nucleus, spectrum of suspected double nucleus (Arp 12) shows object NW is a star. Oval distortion. Spectra unlike all others observed; emission very intense in nucleus, extremely weak elsewhere. Steep nuclear velocity gradient.

NGC 3495.—Curious asymmetrical knotty disk with spiral more extended on N and E; most likely due to galactic extinction, for $\Delta m_b = 0.79$ (Burstein and Heiles 1979) even though $b = +55°$. Nuclear velocity gradient -7.2 km s^{-1} arcsec^{-1} in PA 20°, -0.6 in PA 110°. Rotational velocities moderately symmetric, with faster than Keplerian fall $5 < R < 7$ kpc especially prominent across NE arm. Emission in outermost SW arm more intense than in nucleus.

NGC 1087.—Diffuse messy structure at small R; multiarmed spiral defined at large R by dust lanes. Nuclear emission strong, [S II] $\geq$ [N II] λ6583.

UGC 3691.—Highly obscured, $b = +10°$, $\Delta m_b = 0.62$ (Burstein and Heiles 1979). Spiral arm on E well defined by string of H II knots; W part of galaxy almost totally obscured. Rotation curve symmetrical about obscured nucleus; emission strongest off nucleus to E. [S II] > [N II] λ6583.

NGC 4682.—Well defined nucleus, global few-armed spiral. Rotation curve moderately asymmetrical, with negative gradient in prominent knot SW. Emission from knot more intense than from nucleus.

NGC 3672.—Multiarmed attractive spiral, small nucleus, whose rotation axis is not aligned with rotation axis of outer disk (Paper 1). Continuum weak, Hα strong in nucleus and arms. Extremely shallow nuclear velocity gradient (i.e., low mass nucleus), and very asymmetrical rotation curve.

NGC 1421.—Two-armed open spiral seen at high inclination may have small bar. Extremely asymmetrical velocities, with sharp peak followed by fall near 3 kpc NE. Here, NE arm crosses slit tangentially; excess positive velocity corresponds to inward streaming motions, perhaps 20 km s^{-1} depending upon geometry.

NGC 2715.—Stellar nucleus, well defined global spiral, with oval nuclear region. Steep nuclear velocity gradient. Rotation curve to $R = 7$ kpc has been determined by van der Kruit and Bosma (1978). Velocity decrease is faster than Keplerian $10 < R < 14$ kpc, followed by positive velocity gradient, 40 km s^{-1} in 4 kpc, across prominent outer arms. Due to large undulations in rotation curve, V_{max} adopted as 215 km s^{-1} from the smoothed rotation curve.

NGC 4321.—Brightest spiral in Virgo, with spectacular global spiral pattern which continues to nucleus with prominent H II regions and complex spectra (see Fig. 1). Spectra in three position angles show steep nuclear velocity gradient, strong stellar nuclear continuum, and [N II] $\geq$ Hα in nucleus. Numerous velocity asymmetries. Velocity complexities near nucleus make it difficult to establish major axis, but $\phi = 155 \pm 20$ predicts gradients observed in PA 35°, 110°, and 140°. Our result contradicts rotation curve with falling velocities and $\phi = 110°$ (van der Kruit 1973). Angular diameter of NGC 4321 is larger than slit, so outer 25% of galaxy is unobserved. A complete velocity study of this galaxy would be worthwhile.

IC 467.—Global spiral, perhaps weak bar. Emission in several outer knots is more intense than in nucleus. Velocities decreasing faster than Keplerian at $12 < R < 15$ kpc NE, across interarm region. Bright companion at about 9 diameters.

NGC 7541.—Pair with NGC 7537 at one diameter. Barred, two-armed global spiral; poor velocity symmetry, steep nuclear velocity gradient. Complex nuclear velocities are double and triple valued, with emission knots at high and low velocities distinct from nuclear emission (Fig. 4*c*). Weak nuclear continuum, strong emission in outer regions.

NGC 7664.—Nuclear regions very high surface brightness; outer spiral structure weak. Nuclear continuum moderately strong, Hα almost absent in nucleus, and [N II] > Hα; beyond nucleus, emission strong with Hα > [N II]. Steep nuclear velocity gradient $= -31.4$ km s^{-1} arcsec^{-1} in PA 6°.2. Outer region very asymmetric, rotation curve undefined from $15 \lesssim R \lesssim 25$ kpc. $V_{max} = 203$ km s^{-1} adopted.

NGC 2998.—Well defined two-armed global spiral. Moderately strong nuclear stellar continuum with [N II] > Hα. [N II] nuclear emission broad. Hα (arms) > Hα (nucleus); [N II] (arms) < [N II] (nucleus). Velocity gradient $+56$ km s^{-1} arcsec^{-1} in PA 53°, -0.7 in PA 143°. Positive velocity gradient across each arm, with just marginally non-Keplerian velocity fall between arms, where emission is not detected. $V_{max} = 215$ km s^{-1} from smoothed rotation curve.

NGC 753.—Well defined two-armed global spiral with compact nucleus. Moderately strong stellar nuclear continuum, [N II] > Hα; extremely weak [S II] may be due in part to decreasing spectral response of image tube + grating, although grating blazed at 8032 Å would not be expected to show marked decrease. Steep nuclear velocity gradient. Exposure terminated after 1^{h}; a longer exposure would probably extend to larger R.

NGC 801.—Close to edge-on; spiral structure poorly discerned. Moderately strong stellar continuum, but Hα > [N II]; [S II] relatively weak. Velocity gradient $+43$ km s^{-1} arcsec^{-1} in PA 150°, $+1.3$ in PA 49°.1. Strong emission line compact galaxy 79″ SW with $V_0 = 14{,}820 \pm 25$ km s^{-1}.

UGC 2885.—Stellar nucleus, two-armed global spiral. Strong nuclear stellar continuum with intense [N II] emission; [N II] > Hα; [S II] weak. Velocity gradient 102 km s^{-1} arcsec^{-1} in PA 43°.2, -0.2 in PA 140°; third spectrum (PA = 40°) shows only minor differences from that in PA 43°.2. As rotation curve remained approximately flat at $\sim$280 km s^{-1} for more than 50 kpc, V_{max} adopted as 280 km s^{-1}.

Catalogue (Sandage and Tammann 1980, RSA), the *Second Reference Catalogue of Bright Galaxies* (de Vaucouleurs, de Vaucouleurs, and Corwin 1976, RC2), and the *Uppsala General Catalogue* (Nilson 1973, UGC) to satisfy the following criteria: classification Sc in the RSA (SBc and Sbc excluded); inclinations greater than 50° so that uncertainties are minimized in transforming from velocities on the plane of the sky to circular velocities in the plane of the galaxy; and angular diameters d between 2.'2 and 5.'5, so as to match the length of the spectrograph slit. Additionally, we required that the linear diameters of the set of galaxies span the range of Sc galaxy linear diameters, so as to exploit the known correlation of diameter and luminosity. To meet these conditions, intrinsically small galaxies tend to be nearby (so as to have sufficiently large angular size), while intrinsically large galaxies are all at greater distances (so as to have small angular size). This correlation of size with distance is, of course, an artifact of our selection requirements for the sample, and not a property of the galaxies. We also wish to emphasize that the distribution in sizes for the Sc galaxies in this set reflects our selection of galaxies having a large range in radii, rather than a distribution of radii in a fixed volume of space. The galaxies chosen for study are almost all little known, previously unstudied Sc's; four of them are not included in the RC2, but are classified Sc in the UGC.

II. OBSERVATIONS

Galaxies included in this study are listed in Table 1, column (1), arranged according to increasing linear radius. For each galaxy, spectra at high velocity dispersion (25 Å mm^{-1}) and high spatial scale (25″ mm^{-1}) were obtained with the slit of the spectrograph aligned along the major axis; for some galaxies, a minor axis spectra was also obtained. The galaxies were observed with the Kitt Peak 4 m RC spectrograph which incorporates a Carnegie image tube, except for NGC 3672 which was observed at Cerro Tololo with equivalent instrumentation, but at 50 Å mm^{-1}. Except for five galaxies discussed in Papers I and IV, all observations were made in 1978 December. Exposure times were generally 2^h to 3^h for major axis plates, and less for minor axis plates (to save time). Position angles for the slit are listed in column (6); major axes are determined dynamically if two or more spectra are available; otherwise they are measured from the Palomar Observatory Sky Survey (POSS) prints.

We show in Figure 1 (Plate 17) reproductions of all major axis spectra. As can be seen from an examination of the spectra, no galaxies show velocities which decrease significantly at large nuclear distances. On the contrary, most galaxies exhibit rotational velocities which are increasing to the edge of the optical galaxy. For this sample, rising rotation curves are the general rule. Figures 2 and 3 (Plates 18 and 19, respectively) are photographs of the galaxies. The photographs come from image tube plates taken with the 72 inch (1.8 m) telescope of the Ohio State and Ohio Wesleyan Universities at Lowell Observatory, the KPNO and CTIO prime focus, reproductions from the POSS, and Polaroid copies of the KPNO TV screen which displays the slit. This plate material is unsuitable for a study of luminosity profiles for these Sc's, but we are presently obtaining calibrated direct plates.

Because of the high dispersion, only a limited wavelength range is covered: emission lines of Hα, [N II] λλ6548, 6583, and [S II] λλ6717, 6731 are observed. At this high scale, the emission is generally discontinuous; intense where bright H II knots in the arms are viewed by the slit, and weak in the interarm regions. All spectra were measured on a Mann two-dimensional measuring engine at the Department of Terrestrial Magnetism (DTM) by Rubin. Hα and [N II] were routinely measured, but [S II] only where Hα or [N II] lines were confused with night sky lines. Velocities are calculated in the optical convention: $V \equiv cz = c(\lambda - \lambda_0)/\lambda_0$. The internal accuracy of a single measure is about ± 3 km s^{-1}. For the spectra obtained in 1978 December, the night sky lines are used as comparison lines, to establish both the wavelength scale and the curvature across the slit. Because the optical path for the night sky and the galaxy emission is identical, night sky lines should ultimately define a more accurate wavelength scale than that of the neon-argon comparison spectrum applied at the telescope. Identifications and wavelengths of the night sky OH lines are from Bass and Garvin (1962) as tabulated by Peterson *et al.* (1976). After completion of our reductions, B. T. Lynds (1979) informed us that some OH wavelengths should be decreased by 0.2 or 0.3 Å. Thus, the central velocities determined with respect to the night sky lines may be too low by about 10 or 20 km s^{-1}. Such velocities are indicated by an asterisk in column (4).

Additional evidence that the optical velocities are systematically low comes from a comparison of the optical velocities (col. [3]) with the 21 cm velocities. For 13 galaxies in our sample, 21 cm velocities are available (Paper IV; Thonnard *et al.* 1978; Shostak 1978). For eight galaxies with optical velocities determined from wavelengths of night sky lines, the difference is $\Delta(V_{opt} - V_{21}) = -20 \pm 5$ km s^{-1}, but only -7 ± 3 for five galaxies with velocities based on neon-argon comparison lines. Because the proper form for the correction to the OH wavelengths is not yet established, we have not applied such a correction here. It would not affect the rotational velocities, but would increase the distance scale generally less than 1%. The estimated errors in column (3) come from a consideration of measuring errors and symmetry of the rotational velocities, but do not include the error due to the adopted OH wavelengths.

For each galaxy, the measured heliocentric velocities on the plane of the sky, as a function of angular distance from the nucleus, are shown in Figure 4. For this illustration, only the Hα measures have generally

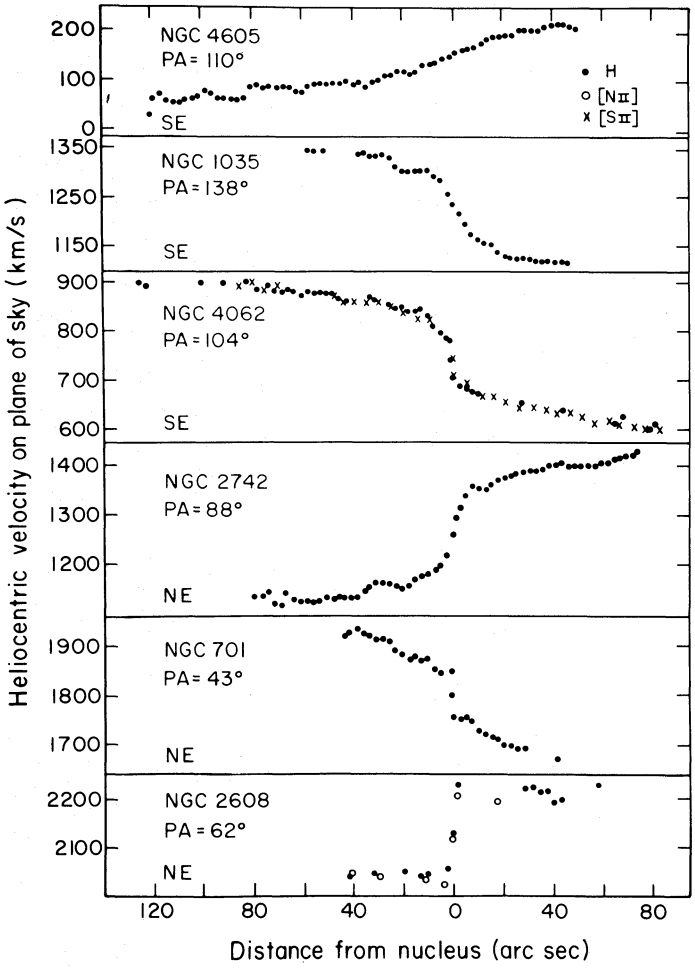

FIG. 4.—Heliocentric line-of-sight velocities on the plane of the sky as a function of angular distance from the nucleus for 21 Sc galaxies. Generally, only velocities from Hα are plotted, to reduce confusion on diagrams.

been plotted, to reduce the confusion. The velocity undulations extending over about 10 kpc are assumed to be real, based on the excellent agreement between velocities from all measured lines. The center of symmetry of the velocities is adopted as the systemic velocity, V_0, of the galaxy; this value (col. [3]) is corrected for the motion of the Sun with respect to the Local Group (column [4]). A distance for each galaxy (col. [5]) is derived from its corrected velocity, assuming $H = 50$ km s^{-1} Mpc^{-1}. For any other value of H given by $H = 50h$, the linear radii of all galaxies scale by $R(H = 50)/h$. Most of the galaxies are not in de Vaucouleurs groups (1975) or in Zwicky (Zwicky and Kowal 1968) clusters; no attempt was made to derive cluster distances for those in clusters.

Emission is detected and measured, in the mean, to 83% of the radius of each galaxy. In column (9), we list the angular radius of each galaxy out to the 25 mag arcsec^{-2} isophote (RC2), and the corresponding linear radius in column (10). This value is affected both by inclination (which makes the galaxy apparently larger) and by foreground galactic extinction (which makes the galaxy apparently smaller). The proper forms for these corrections are still uncertain; those in RC2 are adequate for galaxies with only little extinction. Instead, we have adopted extinction corrections Δm_b (col. [11]) and corrections to the radii of the form suggested by Burstein and Heiles (1979) and Burstein (1980) and notes to Table 1. A justification for this form comes from our few galaxies at low galactic latitude ($|b| < 15°$), which are observed through about 1 mag extinction. Based on the adopted corrections, the radii out to 25 mag arcsec^{-2} lie outside the image detectable on the Palomar Sky Survey prints, and beyond the last detected emission knots, which seems reasonable. With the smaller RC2 corrections, the corrected radius often lies within the optical image and is smaller than the radius of the last detected emission, which seems less reasonable. However, for either form, the corrections to the radii are small and do not affect the rotation curves. The corrected radii, $R^{i,b}$, are tabulated in column (12). The radius to the farthest

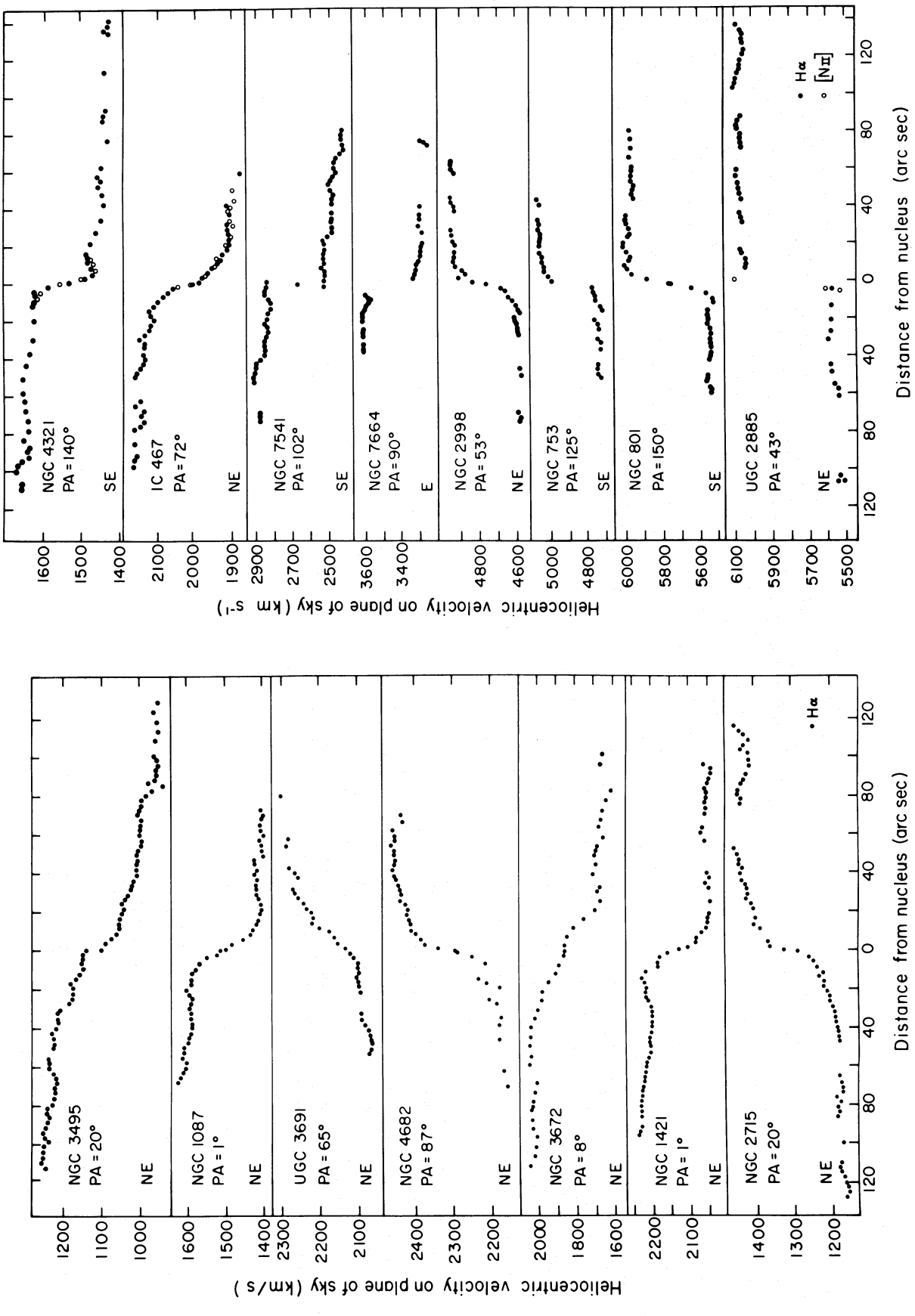

FIG. 4.—*Continued*

measured velocity, R_f, is listed in column (13), and the ratio of the two, $R_f/R^{i,b}$, in column (14). Only for three galaxies is the coverage less than 70%: NGC 753 (55%), 709 (61%), and UGC 2885 (67%). Except for UGC 2885, the largest Sc we have identified, additional observations would add little to our conclusions.

Radial velocities for 13 of these galaxies are listed in RC2. The mean difference $|V_{RC2} - V_{here}| = 81 \pm 25$ km s^{-1}. For NGC 1087, the published velocity differs by +321 from our value. Once again, we stress that large velocity errors permeate existing catalogs.

III. THE ROTATION CURVES

We assume that the emission arises from H II regions which are moving in planar circular orbits about the center of each galaxy. The observed line-of-sight velocities along the major axis can then be projected to velocities in the plane of each galaxy, with $V(R) = (V_{obs} - V_0)/\sin i$. For galaxies for which the major axis ϕ is displaced from the position angle of the spectrum, η, the circular velocity is given by

$$V(R) = \frac{(V_{obs} - V_0)[\sec^2 i - \tan^2 i \cos^2(\eta - \phi)]^{1/2}}{\sin i \cos(\eta - \phi)},$$

$$R = s[\sec^2 i - \tan^2 i \cos^2(\eta - \phi)]^{1/2},$$

where s is the nuclear distance on the plane of the sky and R is the nuclear distance in the plane of the galaxy. Values for ϕ and i are listed in columns (7) and (8) of Table 1. The adopted rotation curve is formed from both sides of the major axis. In general, velocities are reasonably symmetrical on both sides of the major axis; the principal exceptions are NGC 3672, 1421, 4321, and 7541. A simple way to determine the symmetry properties of the velocities is to trace a smooth curve through the points in Figure 4, then rotate the tracing paper 180° about the origin and compare the traced line with the plotted points. The adopted rotation curves are plotted in Figure 5, arranged by increasing linear radii, and the velocities are listed in Table 2.

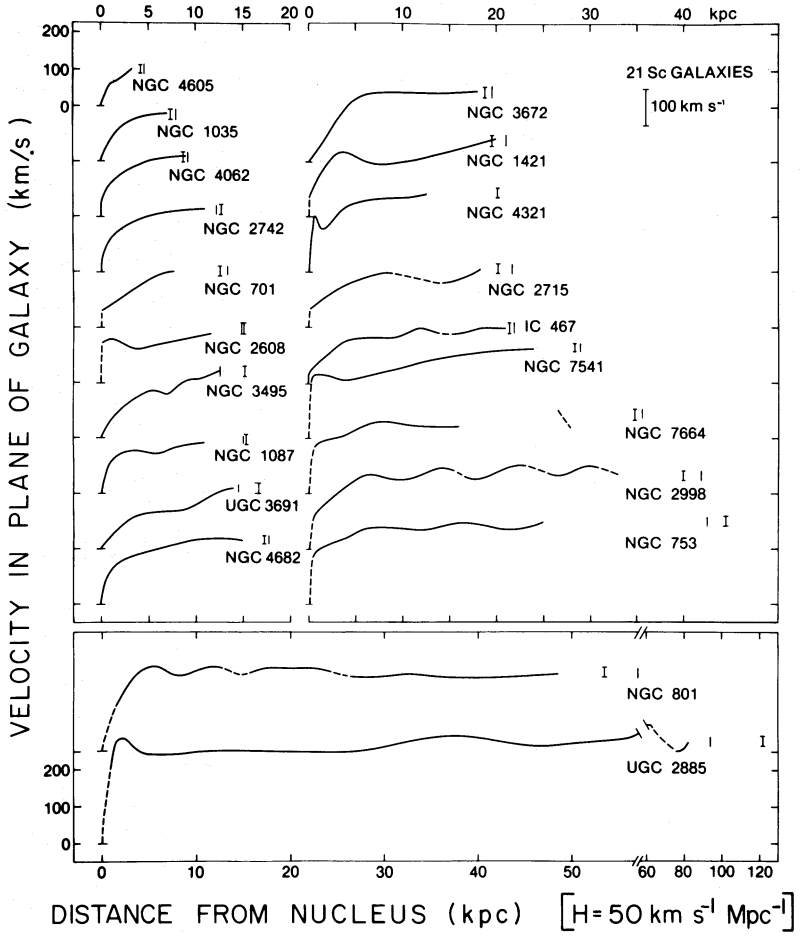

FIG. 5.—Mean velocities in the plane of the galaxy, as a function of linear distance from the nucleus for 21 Sc galaxies, arranged according to increasing linear radius. Curve drawn is rotation curve formed from mean of velocities on both sides of the major axis. Vertical bar marks the location of R_{25}, the isophote of 25 mag arcsec^{-2}; those with upper and lower extensions mark $R^{i,b}$, i.e., R_{25} corrected for inclination and galactic extinction. Dashed line from the nucleus indicates regions in which velocities are not available, due to small scale. Dashed lines at larger R indicates a velocity fall faster than Keplerian.

1980apj...238..471r

TABLE 2

VELOCITIES IN PLANE OF GALAXY (km s^{-1})

R_{kpc} \ NGC4605	1035	4062	2742	701	2608	3495	1087	U3691	4682	3672	1421	2715	4321	I467	7541	7664	2998	753	801	U2885	⟨V⟩±m.e.
0	0	0	0	0	0	0	0	0	0	0	0	0	0	0	0	0	0	0	0	0	
0.5	37	41	70	68	52	115	35	50	19	62	14	75	58	135	41	168	-	88	140	-	-	70±10
1.0	58	59	91	83	60	117	53	87	34	87	32	102	71	133	53	168	137	103	149	-	208	94±10
1.5	66	74	102	104	68	116	68	100	47	101	52	127	82	114	67	167	142	115	156	123	272	108±11
2.0	69	87	113	116	78	112	77	108	58	112	71	149	91	124	79	167	145	126	160	154	287	118±11
2.5	80	98	122	126	86	105	87	114	69	119	92	163	98	140	84	167	149	136	163	177	285	127±11
3	93	108	128	133	94	98	98	117	79	124	117	171	103	158	97	167	153	145	167	193	270	134±10
4	(101)	119	142	142	112	93	115	117	92	133	152	174	115	182	112	167	164	167	177	218	251	147±9
5		122	153	150	129	98	126	114	91	143	173	163	127	188	121	168	174	187	192	232	241	155±9
6		126	158	157	143	103	131	110	96	151	182	151	135	190	127	171	185	203	207	228	239	160±9
7		128	160	161	151	108	[120]	119	103	158	184	146	142	193	128	175	193	198	206	216	239	161±9
8			162	164	(150)	113	143	125	108	164	185	146	147:	197	127	182	194	190	204	208	242	167±9
9			163	167		118	162	132	111	169	187	149	147:	199	129	188	191	187	203	212	244	170±8
10				169		123:	158	137	122	173	188	152	144	201	132	194	186	190	202	220	246	173±9
12				(171)		(132)	173	(140)	128	178	191	162	133	204	152	208	183	204	204	230	250	186±9
14							179		134	172	192	175	[121]	208	[137]	219	183	219	216	[213]	250	187±10
16										(168)	192	183	133	(210)	138	225	(183)	205	220	218	250	193±13
18											(192)	197	157		151	232		194	213:	225	250	202±12
20												208	(160)		152	239		212	205	228	250	213±12
22															(152)	242		228	207	226	250	231±7
24																(247)		219:	216	220	250	226±8
26																	(230)	211:	(221)	[209]	250	225±10
28																	187	206		203	255	213±15
30																		222		204	263	230±17
32																		215		212	274	234±20
34																		209		208	283	233±25
38																				202	285	244±42
42																				204	275	240±36
46																				208	268	238±30
48																				(211)	270	
52																					279	
56																					283:	
62																					321	
66																					[289]	
70																					[275]	
74																					[259]	
78																					262	
82.3																					273	

Notes: : No measured emission within 1 or 2 kpc of this point; tabulated velocity is just an interpolation between nearest velocities.

[] Velocity decrease to this R is faster than Keplerian, i.e., $V_j(R_j)^{1/2} > V_k(R_k)^{1/2}$. This would require negative density, and ∫ mass decreasing with R. More realistically, non-circular streaming motions must be present.

() Last measured point occurs at R slightly before R listed in table. See Table 1, Column 13, for exact R_f.

In general, the rotation curves are characterized by velocities increasing with radius; only the largest galaxies have rotation curves which are flat. Thus, the small Sc's exhibit in their rotational properties the same lack of Keplerian decreasing velocities as do the high-luminosity galaxies (Paper IV). In many galaxies, positive velocity gradients are observed across a spiral arm; velocities on the inner edges are often tens of km s^{-1} lower than velocities on the outer edges. Significantly, the velocity decrease from the outer edge of one arm to the inner edge of the next arm is faster than Keplerian in some regions of five or six galaxies, i.e., faster than $R^{-1/2}$. This is compelling evidence that noncircular velocities are present, in violation of our initial assumption of only circular orbits. Regions of faster than Keplerian fall are indicated by dashed lines in Figure 5. Smoothed rotation velocities for these regions are listed in Table 3. Based on this obvious evidence of noncircular motions, it is likely that noncircular motions have gone undetected in other regions. Their effects on our other conclusions should be small, and all other observed velocities, projected to the plane, are assumed to be rotational velocities.

For each galaxy, we adopt a value for V_{max}, the maximum rotational velocity, from the smoothed rotation curves. Values for V_{max} are tabulated in the final column of Table 1. For 16 galaxies, the maximum rotational velocity is observed at the last measured point; i.e., the rotation curves are still rising, albeit slowly, at the limits of the observations. Following the general notes to Table 1, we record a few notes about the morphology, the line ratios, the rotational symmetry, and the nuclear gradients in each galaxy.

Several sources of uncertainty affect the adopted rotation curves: (1) linear distance scales will change by a common factor if the value of H is altered uniformly; (2) peculiar motions for each galaxy will introduce individual scale changes; (3) a peculiar motion for our Galaxy will produce values of H which differ in different directions and will alter each linear distance scale depending on the angular distance of each galaxy from the apex of our Galaxy's motion. Only for the few nearest galaxies will peculiar motions produce a significant change. For NGC 4606 ($V_c = 288$ km s^{-1}), the adopted scale is highly uncertain. However, even if H differs by as much as a factor of 2 in different directions, the properties of the rotation curves and the conclusions of our study will not be substantially altered. The principal source of error in the rotational velocities, the projection factor to the plane, should be minimized by our observations of highly inclined galaxies. Only for NGC 4321 is the viewing angle low. This galaxy was added to our sample because of indications (van der Kruit 1973) that it might have a falling rotation curve. Our observations do not support this conclusion; see notes for NGC 4321.

IV. COMMON PROPERTIES OF Sc ROTATION CURVES

The optical rotation curves shown in Figure 5 represent the most extensive uniform material available from which to deduce the dynamical properties of disk galaxies with small bulges. In particular, these galaxies span an enormous range in radius, with $R^{i,b}$ extending from 4 to 122 kpc; this corresponds to a range of luminosity from -18 to -23. Although each rotation curve is unique, some remarkable similarities do emerge, which can be employed to characterize broadly the rotational properties of Sc galaxies.

Beyond the nucleus, all galaxies, big and small alike, share a surprisingly similar pattern of velocity variation with R (*R on a linear scale*). Velocities rise rapidly within about 5 kpc, and more slowly thereafter; rotation curves are flat only at very large R. *None* of the rotation curves have the "classical" shape, adopted so frequently in the past, of a long nearly Keplerian drop in velocity after the initial rapid rise. Moreover, the scatter between the rotation curves of individual galaxies is correlated with galaxy radius; small galaxies have velocities, at a given R, which are

TABLE 3

SMOOTHED ROTATION CURVES FOR REGIONS OF FASTER-THAN-KEPLERIAN VELOCITY DECREASES

NGC 3495		NGC 2715		IC 467		NGC 2998		NGC 801		UGC 2885	
R (kpc)	V (km s^{-1})	R (kpc)	V (km s^{-1})	R (kpc)	V (km s^{-1})	R (kpc)	V (km s^{-1})	R (kpc)	V (km s^{-1})	R (kpc)	V (km s^{-1})
4	115	7	142	9	129	10	189	9	212	54	270
5	123	8	143	10	134	12	200	10	218	62	280
6	125	9	143	12	139	14	203	12	222	↓	
7	136	10	141	14	142	16	206	14	218	84	280
8	144	12	133	16	145	18	209	16	218		
9	152	14	125	18	151	20	211	18	225		
10	159	16	133			22	213	20	228		
12	173					26	214	22	225		
						30	215	24	221		
						34	216	26	216		
								28	212		
								32	207		
								36	205		
								40	202		

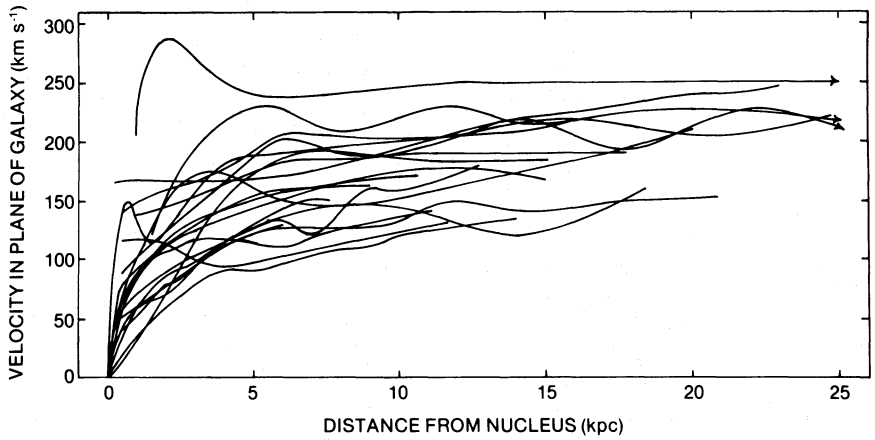

FIG. 6.—Superposition of all 21 Sc rotation curves. General form of rotation curves for small galaxies is similar to initial part of rotation curve for large galaxies, except that small galaxies often have shallower nuclear velocity gradient and tend to cover the low velocity range within the scatter at any R.

typically lower than those of the large galaxies at the same R. Thus, small galaxies have lower values of V_{max} then large galaxies for two reasons: (1) although they share common parts of the general Sc rotation curve, small galaxies do not extend to large R where the velocities are highest, and (2) within the scatter about the mean, the small galaxies occupy the low velocity range. These characteristics are shown in Figure 6, where we have superposed all of the rotation curves. The common form for all rotation curves, the relatively small spread in V at any R, and the propensity for the small galaxies to have lower V are apparent. The mean rotational velocity as a function of radius for all Sc galaxies in our sample is plotted with the solid line in Figure 7 and listed in the last column of Table 2. This we call the common Sc rotation curve.

The astronomical literature abounds with rotation curves for Sc galaxies which deviate significantly from the common Sc rotation curve found here. Only in a few peculiar objects is this discrepancy probably real. In most cases, the rotational velocities come from plates of much lower dispersion than used here (often 15 times lower), smaller spatial scale, and for galaxies of lower inclination, leading to a highly uncertain value for V_{max}. Equally important, most published optical rotation curves extend only to small R (typically ~ 10 kpc) and thus sample only the dynamics of the inner galaxy. Sc galaxies M51 and NGC 4321 both

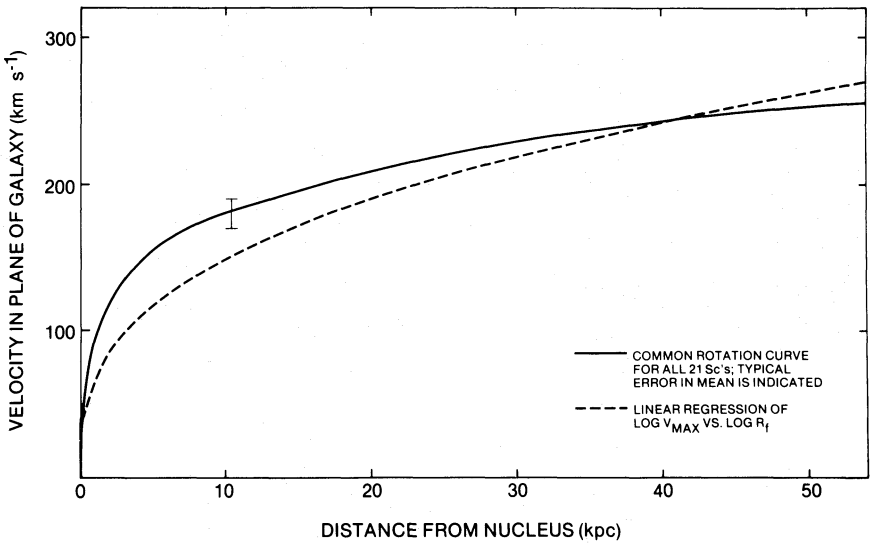

FIG. 7.—Rotational velocity as a function of radius for all 21 Sc galaxies. Solid curve is the mean rotational velocity at any given radius for all Sc galaxies; the common Sc rotation curve. Dashed line is the solution to eq. (1); the mean of the two least square linear regressions of log V_{max} (the maximum rotational velocity of a single galaxy) versus log R_f (the farthest measured velocity in that same galaxy) for all 21 Sc galaxies, i.e., the Tully-Fisher (1977) relation on a linear scale. This curve is replotted in the more familiar log R versus log V_{max} form in Fig. 7. The similarity between the common Sc rotation curve and the Tully-Fisher relation is striking.

serve as examples of the inclination problem. For NGC 4321, the low inclination has led to both discrepant values of V_{max} (Sandage and Tammann 1976; Tully and Fisher 1977) and a difficult choice of the major axis. Our plates in three position angles suggest a major axis 45° from that adopted previously (van der Kruit 1973). For M51, the extensive recent study by Goad, de Veny, and Goad (1979) has obtained velocities of high accuracy over the inner half of the galaxy (170″ = 7.9 kpc). Their data show a rotation curve with $V_{max} = 250$ km s^{-1}, about 100 km s^{-1} higher than the common curve. However, M51 is so close to face-on that its inclination is uncertain. Following Tully (1974), Goad *et al.* adopt $i = 20°$. Had they chosen $i = 35°$ (as did Burbidge and Burbidge 1964), then $V_{max} = 140$ km s^{-1}, in agreement with the velocity predicted by the common curve. For normal Sc galaxies of low inclination, it may be wiser to determine an inclination from an observed rotation curve or 21 cm profile velocity width and the common rotation curve than to attempt to obtain it from the form of the spiral arms.

Small galaxies have low maximum rotational velocities; large galaxies have high rotational velocities. The relation between V_{max} and $R_{Holmberg}$ (R_H) has been discussed earlier by Tully and Fisher (1977, TF) as one representation of the TF relation. TF use the width of the 21 cm profile, ΔV; it is assumed that ΔV measures twice the peak of the rotation curve. The more widely used form of the TF relation, V_{max} versus absolute magnitude M, will be discussed in a later paper (Rubin and Burstein 1980). The discussions generated by their discovery (Sandage and Tammann 1976; Fisher and Tully 1977; Roberts 1978; Aaronson, Huchra, and Mould 1979) have been directed generally toward the (V_{max}, M)-relation. Here we examine the (V_{max}, R)-correlation.

For the 21 Sc galaxies studied, the increase of the maximum rotational velocity, V_{max}, with increasing galaxy radius (and indeed the form of the common rotation curve) is well represented by a straight line on a log V_{max}, log R plot. In Figure 8, we plot log V_{max} versus log R_f; the line drawn is the mean of the two least squares regression lines and is given by:

$$\log R_f = -5.07 \pm 0.55 + (2.80 \pm 0.27) \log V_{max}\,, \qquad r = 0.86\,, \quad (1)$$

$$R_f \propto V_{max}^{2.8 \pm 0.3}\,. \quad (2)$$

Equation (1) is also plotted as the dashed curve in Figure 7. The correlation confirms the previous discussion: the relation of V_{max} and R_f can be understood in terms of the small scatter about a common rotation curve for Sc galaxies, a curve which can be approximated by a straight line on a log, log plot, with the smaller galaxies extending only to smaller R. From equation (1), we evaluate V_{max} for various sized Sc's: $V_{max} = 150$ km s^{-1} for galaxies with $R = 10$ kpc; $V_{max} = 200$ km s^{-1} for $R = 25$ kpc; and $V_{max} = 300$ km s^{-1} for $R = 70$ kpc. We stress here that because of the strict dependence of V_{max} on linear size of the galaxy, quoting a mean V_{max} for Sc galaxies is of very limited validity, for the value is dependent on the size distribution of the sample.

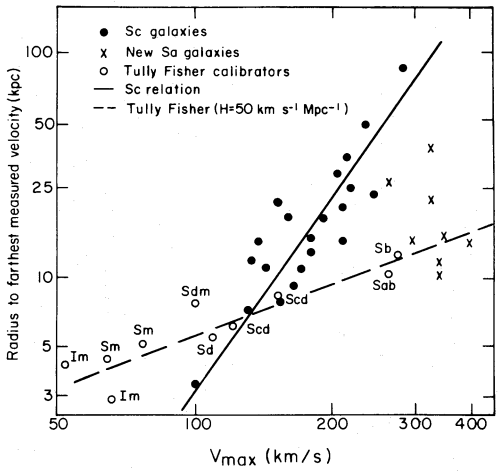

FIG. 8.—R_f, the radius to the farthest measured velocity, versus V_{max}, the maximum rotational velocity, for 21 Sc's (*filled circles*), plotted here on a log, log scale. The solid line is the mean of the two least squares linear regression lines. The crosses show the location of 8 Sa galaxies we are presently studying. The open circles show the 10 calibrating galaxies of Tully and Fisher, marked with their Hubble types. The dashed line, the mean of the two linear regression lines for the Tully-Fisher data, indicates a much less steep relation than the Sc's. Because very late type galaxies have very low V_{max}, and early Hubble types have high V_{max}, a mixture of various types will produce a biased relation.

The line defined by equation (1) is *not* the line which TF derive for the calibrating galaxies. For 10 nearby calibrating galaxies of Hubble classes Sab through Scd and irregular, and with well determined distances, the relation between log R_H and log V_{max} which they derive is significantly less steep than that found here for the Sc's:

$$\log R' = 0.56 \pm 0.15 + (0.76 \pm 0.09) \log (\Delta V/2)\,, \qquad R = 0.91\,,$$

$$R' \propto (\Delta V/2)^{0.76 \pm 0.09}\,.$$

Their data points and this line are plotted in Figure 8; the line is the mean of the two regressions which we have calculated (they did not make least squares fits). In transforming from R_H to R' (i.e., an artificial R_f), we have adopted the relation $R' = R_f = 0.6R_H$, i.e., our farthest observation extends generally to 60% of the Holmberg radius. This relation comes from a comparison of the radii of eight Virgo cluster galaxies studied by Holmberg (1958) and used by FT; for these galaxies, $R_{25} = 0.72R_H$. Additionally, four of our Sc galaxies have R_H measures; for these, $R = 0.69R_H$. Hence, $R_{25} = 0.7R_H$, and $R_f = 0.83R_{25}$. It is immediately clear that the slope defined by the TF galaxies is not the slope defined by the Sc galaxies. (Note that an increase in the adopted value of H will

raise the line relative to our sample, but the slopes will be unaltered.)

It is likely that the discrepant slope from the TF galaxies arises from the small range in radius and the large range in Hubble types they encompass. Eight of their calibrators are irregulars, dwarfs, Sd's or Scd's; all are small with $R_{25} < 10$ kpc and $V_{max} < 150$ km s^{-1}. The other two galaxies are an Sab and Sb with $R_{25} < 18$ kpc, but with high V_{max}, $V_{max} \sim 275$ km s^{-1}. However, earlier Hubble types are known to have larger values of V_{max} (Paper IV; Roberts 1978). Thus, when TF use as calibrating galaxies these two galaxies with V_{max} near 300 km s^{-1}, their radii are less than half that of an Sc with an equivalent V_{max}. For an Sc to have V_{max} as high as that for an Sa or Sab galaxy, the Sc galaxy must be enormous. To emphasize this point, we show in Figure 8 preliminary results from our current observations of rotational velocities of Sa galaxies by plotting V_{max} versus R_f for eight Sa's in which emission was detected in the mean to 81% of the radius of each galaxy. All Sa's which we have observed have high V_{max} values, regardless of galaxy size. Thus, a mixture of small late type galaxies and a few early types will produce a significantly smaller slope for the correlation of V_{max} with R, and can account for the TF result. In Figure 9, we show V_{max} versus Hubble type for the Sc's, Sa's, and the galaxies discussed earlier (Paper IV). The separation of V_{max} for Sc's and Sa's is remarkably clear. Thus, we reiterate even more strongly the caution which Roberts (1978) has already raised in connection with the correlation of V_{max} with absolute magnitude:

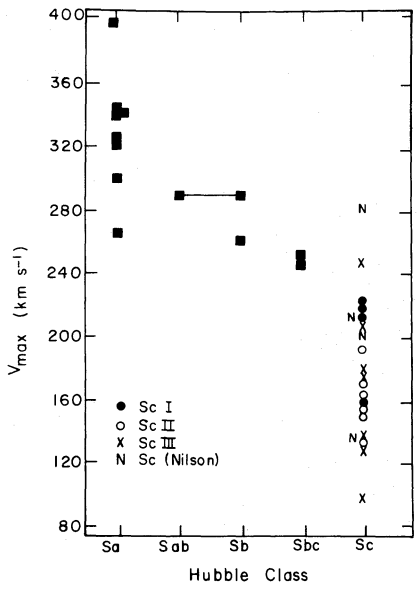

FIG. 9.—V_{max} versus Hubble type for 21 Sc's, 8 Sa's, and several Sb's studied earlier (Paper IV). The Sc luminosity classification shows a general correlation of high luminosity and high V_{max}. Note especially the very high V_{max} values for the Sa galaxies and the very little overlap of V_{max} values for Sa's and Sc's.

because V_{max} is such a strict function of Hubble class, any correlation involving V_{max} should properly be restricted to a small range of Hubble types.

We return to a discussion of the implications of these common features for Sc rotation curves in § VIII.

V. DYNAMICAL AND SPECTROSCOPIC PROPERTIES OF THE CENTRAL REGIONS

Close to the nucleus, the velocity patterns of the galaxies exhibit great individuality, along with some systematic properties which are weakly correlated with galaxy size, and hence luminosity. In the smaller galaxies, there is very often a very gentle increase of velocity with radius over the central region, as in UGC 3691 with $V/R = 37$ km s^{-1} kpc^{-1}. In some galaxies, more often the large ones, rotational velocities are high just a few seconds off the nucleus. For these galaxies, details of the velocity and spatial structure are lost in the nuclear continuum, as in NGC 7541, with $V/R > 560$ km s^{-1} kpc^{-1}. (Here $V = 168$ km s^{-1} at its first measured velocity at $R = 300$ pc.) The steep velocity rise is not a consequence of the smaller spatial scale, as can be seen from Figure 5, where velocities are plotted on a linear scale. Values of central velocity gradients for all program galaxies will be presented later (Rubin and Burstein 1980).

The central angular velocity, V/R, is related to both the central mass (V^2R) and central density (V^2/R^2). Galaxies with large central angular velocities have massive, high-density nuclear regions (as high as 10^{10} $M_\odot$ within 1 kpc). In a few cases, the steep initial rise is followed by a velocity decrease; these galaxies have stellar nuclei.

Nine of the Sc galaxies in our sample were observed by Dressel and Condon (1978) in their 13 cm Arecibo radio continuum survey. Of these nine galaxies, three have shallow nuclear velocity gradients (NGC 4062, 3495, and UGC 3691); the observed flux density at the position of these galaxies was below 15 mJy, the detection limit. The remaining six galaxies (NGC 2608, 4321, 7541, 7664, 753, and UGC 2885) all have steep nuclear velocity gradients, and, for four of these, the observed flux density was considerably greater than their detection limit. Normalizing the observed flux densities to 40 Mpc, the median distance of the nine galaxies observed at 13 cm, the mean upper detection limit for the three galaxies with shallow nuclear velocity gradients is 7 mJy (ranging from 2 to 16 mJy), while for the six galaxies with steep nuclear velocity gradients, the mean flux density is 106 mJy (four detections ranging from 29 to 209 mJy and two upper limits at 16 and 131 mJy). Thus, it appears that a steep nuclear velocity rise is evidence not only for a large nuclear mass, but also for relatively strong radio activity. For comparison purposes, M31, if it were at a distance of 40 Mpc, would have a 13 cm flux density of less than 2 mJy whereas NGC 1275 (Perseus A), if it were at the same distance, would have a flux density of 50 Jy.

Spectroscopically, there is a striking difference between the spectra of some galaxies with shallow central velocity gradients and some with steep gradients. Hα is generally stronger than [N II] in Sc nuclei, just as in conventional H II regions. For five galaxies, however, the Hα/[N II] ratio reverses discontinuously at the nucleus, and [N II] is here stronger than Hα. For these galaxies, NGC 753, 2998, 4321, 7664, and UGC 2885, the character of the emission also changes abruptly where [N II] strengthens, from sharp lines off the nucleus, to diffuse emission in the nucleus. Because the emission is broad along the minor axis as well (Fig. 1, UGC 2885 minor axis), it implies that the emission arises either in high-velocity randomly moving clouds or from a rapidly rotating disk whose radius is smaller than the region sampled by the 1".3 slit. Moreover, these spectra all exhibit intense nuclear continua in the red spectral region, arising from a red stellar population. The cause of the Hα/[N II] intensity reversal in the nuclei of some galaxies remains obscure (Searle 1976). However, the strong [N II] nuclear emission generally in high-luminosity galaxies with massive nuclei, nuclei which show strong red continua, suggests that [N II] intensity correlates with nuclear luminosity, and in turn with the density and velocity properties of the nuclear population. We would expect high velocity dispersions and high bulge luminosities for the galaxies with strong [N II].

In many small, low-luminosity galaxies, the [S II] lines are each stronger than [N II] λ6583. In galaxies of intermediate and large size, the [S II] λλ6717, 6731 lines are generally weaker than [N II] λ6583. In any single galaxy, the ratio of [N II]/[S II] is generally higher in H II knots than in the low-excitation interarm regions; [S II] appears relatively strong in many interarm spots.

In summary, Sc nuclear properties come in a wide variety, but can be discussed in terms of two distinct classes. The majority of Sc's have nuclei whose spectra show weak continua and strong relatively narrow Hα emission. The galaxies tend to be small, of low luminosity, low central mass density, with shallow central velocity gradients, and weak (or undetected) emitters at 13 cm. At the other extreme, a small fraction of Sc galaxies (20% in our sample) show strong, diffuse [N II] nuclear emission, with [N II] stronger than Hα. These galaxies tend to be large, of high luminosity, high central density, steep central velocity gradient, emitters at 13 cm, and to have a large red stellar population. From the population of Sc galaxies with known spectra, the exceptions to this generalization are few; the exceptions tend to be peculiar, or double, or of very high luminosity for their size.

VI. THE RELATION OF GALAXY MORPHOLOGY TO GALAXY DYNAMICS

A major aim of our observing program is to learn how the dynamics of a galaxy influence its morphology. For simplicity, we chose to observe isolated, generally field Sc's, preferably not barred. Since the inception of the program, two factors have caused a major change in outlook. First, a rather novel approach to the study of spiral structure as related to dynamics has been initiated by Kormendy and Norman (1979, KN). Although some of our conclusions will be the opposite of theirs, their approach is such a very major advance in the understanding of spiral morphology that we shall follow it. Second, new plate material indicates that a significant fraction of the program galaxies have (often small) nuclear bars or oval distortions. Hence, the sample contains a wider range of Sc morphological types than had been anticipated. In this section, we discuss briefly the relation of the observed rotation curves to the forms of the spiral structure, to the KN ideas, and to the spiral density wave theory. A study of the detailed dynamics of each galaxy and its relation to the galaxy morphology is presently under way (Kormendy and Rubin 1980).

The spiral density wave theory arose because of the necessity to explain how global spiral structure could persist over many revolutions in a differentially rotating galaxy. More recently, it has become clear that a companion galaxy, or bars or oval distortions in single galaxies, could sustain a density wave even in the presence of differential rotation. Moreover, as KN have stressed, not all spirals show a well defined global spiral pattern; many have short, filamentary arms (NGC 2841 type). These latter galaxies have apparently failed to make a global density wave, and KN suggest that it is because they rotate very differentially. Thus, only a restricted class of spirals requires a spiral density wave theory: isolated galaxies with a global spiral pattern (the "grand design" of Lin) but without bars or oval distortions. Curiously, there are very few such galaxies in our sample. Given only our present program Sc's, the necessity for a spiral density wave theory might not have arisen; bars, ovals, companions, and filamentary nonglobal patterns will account for most of the forms we observe.

However, there is a notable correlation in the sample between the presence of a two-armed spiral pattern and the radius of an Sc: small galaxies preferentially have ragged filamentary arms while large galaxies preferentially have global spiral patterns. Three of the 11 smallest galaxies have a global spiral pattern, while at least seven of the largest 10 have a global spiral form. In a very general way, this may be understood in terms of the form of the rotation curve. In the initial rising portion, the rotation curve is almost, but *not quite*, linear. Any nonlinearity produces a large differential effect: V is a rapidly varying function of R at small R, and $d(V/R)/dR$, which measures the differential effect, is large. Thus, small Sc's, whose radii encompass only the initial portion of the general rotation curve, have undergone many many rotations, all of them very differential. In the absence of a spiral density wave, small Sc galaxies could not maintain a global spiral pattern. On the other hand, for larger galaxies the

differential effect at large R of a flat rotation curve is small [$d(V/R)/dR$ = constant/R^2] and even less for a rising rotation curve. It will take a long time for the spiral pattern to wind up in the outer regions of a large galaxy. For NGC 801, for example, the rotation period is 1.2×10^9 years at $R = 38$ kpc, and only slightly longer, 1.4×10^9 years, at $R = 48$ kpc. Over the outer 20% of this galaxy, the differential effect during a single orbit is not devastating. Points at $R = 48$ kpc advance only 360° + 50° during an $R = 38$ kpc orbital period. Even in the absence of a spiral density wave, a global pattern could persist over large regions at large R for some 10^9 years. If disks of spiral galaxies are young, as some cosmologies now predict, then the winding problem is further minimized for the outer regions of large spirals. We do not mean to overstate the case, because there are exceptions to the general pattern of small filamentary spirals or large global spirals. But the tendency is worthy of note. Our description differs in a major way from KN. They describe inner rotation curves with "almost solid body" as "least differential," and outer regions (for some they show falling rotation curves) as "most differential." In contrast, we consider inner rotation curves very differential, and outer flat ones only slightly so.

Curiously, both the spiral density wave model and the stochastic star formation model have difficulties with very large galaxies. The density wave model can account well for spiral patterns of dimensions 10 or 15 kpc. However, it is generally not possible to pick a single pattern speed which can extend from the inner Lindblad resonance to corotation if this distance is very great, as it is when corotation is placed at the outer H II regions in very large galaxies. For large galaxies, solutions involving several spiral modes may be necessary, or it may be necessary to continue the pattern through corotation, a difficult task theoretically (Bertin *et al.* 1977).

Gerola and Seiden (1978) have demonstrated that stochastic star formation in a differentially rotating disk can lead to the formation of spiral structure; more often the spiral appears of a filamentary type, but the similarity to observed forms is impressive. Seiden and Gerola (1979) have extended their calculations to make a model galaxy for each of the 21 Sc's, using the rotation curves determined here (Table 2). We show in Figure 2 one of their computer generated galaxies; the computer galaxy is a good representation of the actual one. However, their model relies on the differential effect to string out the luminous regions into filaments and arms. Thus, in larger galaxies where the differential effects are small, no significant spiral pattern emerges, and the structure degenerates to a ragged disk. We hope that the extended rotation curves presented here will act as a stimulus for theories of galactic structure, particularly for very large spirals.

The relation between the morphology and the radius of an Sc discussed above is of help in understanding the basis of the van den Bergh (1960) luminosity classification. The van den Bergh luminosity criteria attempt to tell, from only the morphology of the galaxy, whether the galaxy is intrinsically large or small (i.e., of high or low luminosity). Thus, the characterization of the small low-luminosity Sc's as having ill-defined global spiral arms, and the large, high-luminosity Sc's as having prominent spiral structures, conforms in a very general fashion with (1) the definition of the van den Bergh criteria (1960) as modified and applied by Sandage and Tammann (1980), (2) the dynamical effects of the rotational shear, and (3) the observed forms as a function of galaxy radius.

An evaluation of the success of the van den Bergh luminosity classification can be made by examining some properties of the program galaxies as a function of luminosity class: Table 4. For 16 of the Sc's, new luminosity classifications (col. [2], Table 1) are available from Sandage and Tammann (1980). Individual absolute magnitudes, calculated from RC2 magnitudes corrected for inclination and foreground extinction and adopted distances, will be discussed later (Rubin and Burstein 1980). It is clear from Table 4 that the classification has been able to distinguish Sc spirals of highest luminosity, largest radius and highest rotational velocity as Sc I's. However, it has generally failed to separate the lower luminosity galaxies into meaningful subclasses by radii and V_{max}. Even this limited success, however, is of value in statistical studies.

Throughout this program, we have attempted to exploit the relation between linear radius and luminosity, by choosing for study galaxies with a wide range of radii. We show in Table 4 that the mean properties of galaxies, when grouped by radii, exhibit a variety of correlations. The larger galaxies have the brightest absolute magnitudes and highest V_{max} while the smallest galaxies have faintest absolute magnitudes and lowest V_{max}. The correlation with assigned luminosity classification is good only for galaxies of highest luminosity class. Over all, linear diameters could be a useful tool for statistical galaxy studies, analogous to absolute magnitudes as derived from apparent magnitudes and adopted distances.

VII. UGC 2885: THE LARGEST IDENTIFIED Sc GALAXY

Extremely large galaxies can play an important role in our understanding of the origin and evolution of galaxies and the universe. From a survey of all spirals with known velocities (published and unpublished), we have identified UGC 2885 as having the largest dimensions, with $R_{25} = 94$ kpc; corrected for inclination and galactic extinction, $R^{i,b} = 122$ kpc. It is located at low galactic latitude ($l = 160°$, $b = -14°$) and is obscured by more than 1 mag extinction (Burstein and Heiles 1979). Its Holmberg diameter is of the order of $122 \times 2/0.7 = 350$ kpc. UGC 2885 is located 8° or 9° from the center of the Perseus cluster, and a few degrees beyond its borders as defined by

TABLE 4

A. PROPERTIES OF Sc GALAXIES, GROUPED BY MORPHOLOGICAL LUMINOSITY CLASS

Luminosity Class	⟨L.C.⟩	Number	⟨log V_{max}⟩ (km s^{-1})	⟨Radius^{i,b}⟩ (kpc)	⟨Absolute Magnitude⟩	Global/Filamentary (number)
I–I.5	I.1	4	2.32 ± 0.01	31 ± 7	−21.9 ± 0.3	3/1
II–II.5	II.2	6	2.20 ± 0.02	14 ± 2	−20.2 ± 0.2	4/2
III–III.3	III.0	6	2.20 ± 0.06	15 ± 4	−20.4 ± 0.6	2/2
III (III: omitted)	III.0	4	2.13 ± 0.05	11 ± 3	−19.7 ± 0.6	0/2

B. PROPERTIES OF Sc GALAXIES, GROUPED BY RADIUS

Radius^{i,b} (kpc)	⟨Radius^{i,b}⟩ (kpc)	Number	⟨log V_{max}⟩ (km s^{-1})	⟨Luminosity Class⟩	⟨Absolute Magnitude⟩	Global/Filamentary (number)
28–122	54 ± 14	6	2.36 ± 0.02	I.7 ± 0.7	−22.2 ± 0.2	4/0
15–21	18 ± 1	10	2.22 ± 0.02	II.3 ± 0.02	−20.9 ± 0.2	6/3
4–13	9 ± 2	5	2.15 ± 0.04	II.5 ± 0.2	−19.4 ± 0.4	1/3

Zwicky and Kowal (1968). However, it is probably contained in the Perseus supercluster (see Burns and Owen 1979). UGC 2885 has a semistellar nucleus, and a well defined two-armed global spiral pattern extending to the edge of the optical galaxy (Fig. 3).

Some concept of the immensity of this galaxy can be had by noting that its angular dimensions, 5.′5 × 2.′5, are as large as any in our sample, while its systemic velocity, $V_c = 5887$ km s^{-1}, is 5 times as great as the other galaxies of large angular dimension. It is twice as large as any galaxy observed earlier (Paper IV) in our high luminosity (i.e., large) sample. If placed at the distance of the Virgo cluster (20 Mpc), it would subtend 32′, while the largest spirals (and ellipticals) in Virgo are just 12′ (Sulentic 1977). We have identified no other spiral with $R > 75$ kpc. While they undoubtedly exist, spirals of this size are so rare that larger radial velocity surveys will be necessary to identify them. We had observed this galaxy initially at the NRAO 300 foot (91 m) transit telescope (Thonnard *et al.* 1978) as a filler when the Milky Way was overhead; its large velocity was a surprise.

Because of its distance, the spatial resolution in UGC 2885 is poor: 1″ = 572 pc. The first measured velocity off the nucleus, V(1 kpc) = 208 km s^{-1}, implies a mass at least as great as $10^{10}\ M_\odot$ within 1 kpc. All knowledge of the mass distribution within 1 kpc of the nucleus is lost because of the low resolution. In M87, dynamical and luminosity evidence suggest a massive nucleus $5 \times 10^9\ M_\odot$ within 0.1 kpc (Young *et al.* 1978; Sargent *et al.* 1978). Higher scale observations of UGC 2885 will be necessary to describe the mass distribution within 1 kpc to see how the central mass of an enormous spiral galaxy compares with that of a giant elliptical. Our present plate material suggests that the luminosity contrast between the stellar nucleus and the off-nuclear regions is very great (see Figs. 2 and 3).

For UGC 2885, the rotation period is 2×10^9 years at $R = 122$ kpc. The outer regions have undergone fewer than 10 revolutions since the origin of the universe. (This number is independent of the choice for H, for both the age of the universe and the linear dimensions of the galaxy scale inversely with the Hubble constant.) Yet with even so few rotations, the arms are smooth and well developed, and there are no large-scale velocity irregularities in the three position angles for which we have velocities. Large-scale velocity regularity coupled with so few revolutions means that a well ordered global spiral pattern must be established soon after galaxy formation; it cannot be the product of smoothing introduced by many differential rotations. We will attempt to determine the rotation curve of UGC 2885 to even greater radial distances. But even the present observations put important constraints on models of galaxy formation and evolution.

VIII. DISCUSSION AND CONCLUSIONS

We have obtained spectra and determined rotation curves to the faint outer limits of 21 Sc galaxies of high inclination. The galaxies span a range in luminosity from 3×10^9 to $2 \times 10^{11}\ L_\odot$, a range in mass from 10^{10} to $2 \times 10^{12}\ M_\odot$, and a range in radius from 4 to 122 kpc. In general, velocities are obtained over 83% of the optical image (defined by 25 mag arcsec^{-2}), a greater distance than previously observed. The major conclusions are intended to apply only to Sc galaxies.

1. Most galaxies exhibit rising rotational velocities at the last measured velocity; only for the very largest galaxies are the rotation curves flat. Thus the smallest Sc's (i.e., lowest luminosity) exhibit the same lack of a Keplerian velocity decrease at large R as do the high-luminosity spirals. This form for the rotation curves implies that the mass is not centrally condensed, but that significant mass is located at large R. The integral mass is increasing at least as fast as R. The mass is not converging to a limiting mass at the edge of the optical image. The conclusion is inescapable that nonluminous matter exists beyond the optical galaxy.

2. Positive velocity gradients are often observed in crossing a spiral arm. The decrease from the high velocities on the outer edge of one arm to the low velocities on the inner edge of the next arm is sometimes faster than Keplerian. This is compelling evidence of streaming motions in the arms.

3. Within a few kiloparsecs of the nucleus, the galaxies exhibit great velocity individuality, which is weakly correlated with radius. Small galaxies often have shallow nuclear velocity gradients; some large galaxies have steep nuclear velocity gradients, with the observed velocity close to V_{max} at the first measured point off the nucleus. Steep gradients mean high nuclear mass and density; for UGC 2885 a mass $M(1\text{ kpc}) = 10^{10}\ M_{\odot}$ is derived. These galaxies would also be expected to have large velocity dispersion in their central bulges. Galaxies with massive nuclei are also continuum radio sources at 13 cm.

4. Sc nuclear spectra come in two varieties: those with weak red continuum and strong, relatively narrow Hα, as in conventional H II regions; and those with intense stellar continua, and strong usually broad [N II]. These latter (5 of 21) tend to be large galaxies, of high luminosity, steep nuclear velocity gradients, high nuclear mass density, and probably of high nuclear luminosity. We know of no exceptions to the rule that [N II]/Hα > 1 where the red stellar continuum is strong. There is also some evidence that [S II] is stronger relative to [N II] for the smaller, low-luminosity galaxies. At larger radial distances, emission is generally knotty and discontinuous, with line ratios comparable to those in normal galactic H II regions. These characteristics contrast with those of Sa galaxies, in which the emission is generally smooth and continuous.

5. Beyond the nucleus, velocities are suprisingly similar for all galaxies at each R, independent of galaxy size, rising rapidly to about 5 kpc and slowly thereafter. The rotation curves for all Sc's can be superposed on a linear R scale, with no scaling, to form a common rotation curve. That is, velocities for the small galaxies fit on the initial part of the rotation curve for the larger galaxies. Within the scatter, the large galaxies tend to have the higher velocities. The form of the V, R curve is well approximated by a straight line on a log, log plot. This suggests that at least part of the basis for the correlation of V_{max} with R found by Tully and Fisher (1977) is the form of and the concordance of the rotation curves for Sc's. The correlation found here ($V_{max} = 115\text{ km s}^{-1}$ for galaxies with $R = 5$ kpc rising to $V_{max} = 300\text{ km}^{-1}$ for galaxies with $R = 70$ kpc) is significantly steeper than that derived by TF for a sample of galaxies of various Hubble types. Because early type galaxies have substantially higher value of V_{max} as a function of radius than do Sc's, a mixture of Hubble types will lessen the derived relation.

Does the common form for the Sc rotation curves mean that all Sc galaxies, small or large, sit in generally similar potential wells, in which the optical galaxy defines only that region in which matter happens to be luminous? If we could observe beyond the optical image, especially for the smaller galaxies, would the velocities continue to rise, following the curve defined by those galaxies whose luminous matter extends to much larger nuclear distances? Is the luminous matter only a minor component of the total galaxy mass? Observations of neutral hydrogen may enable such questions to be answered. 21-cm velocities extending beyond the optical image exist only for a few Sc galaxies (Bosma 1978; Krumm and Salpeter 1979); these generally show little velocity decrease beyond the optical image. However, for galaxies as large as 50 kpc, the difference between a flat rotation curve and one decreasing as $1/R^{1/2}$ beyond $R = 50$ kpc (i.e., Keplerian, no mass beyond $R = 50$ kpc) is not large. Velocities would decrease only from $V = 250\text{ km s}^{-1}$ at $R = 50$ kpc (for example) to $V = 210\text{ km s}^{-1}$ at $R = 70$ kpc. Accurate 21 cm velocity mapping beyond the optical image will be crucial in determining the outlying mass distributions for these galaxies.

There are two simpler questions which we can hope to also address when more systematic material is available. First, is the ratio of 21 cm to optical diameter a function of the linear optical dimensions? Are small Sc galaxies more likely to have extended radio diameters than large Sc's? Because extragalactic astronomers have traditionally used angular, rather than linear, dimensions, such questions have not been investigated. If all Sc galaxies reside in generally similar potential wells, then it might be expected that intrinsically small galaxies are small only optically and that optically unseen hydrogen disks extend out several optical diameters. Present data are not conclusive. For the seven Sc or SBc galaxies observed at Arecibo by Krumm and Salpeter (1979), the ratio of hydrogen radius to optical radius decreases monotonically with increasing linear radius from $R(21)/R_H = 1.8$ for NGC 672 ($R_H = 15$ kpc) to $R(21)/R_H = 0.94$ for NGC 947 ($R_H = 32$ kpc). However, for these few galaxies the H I disks are still too small to increase the radius of a small galaxy so that it approaches the size of the larger ones.

Second, are there systematic differences in the value of the maximum rotational velocity obtained from 21 cm observations, $V_{max}(21)$, from that obtained from optical observations, $V_{max}(\text{opt})$, which are correlated with radius? If small Sc's preferentially have large hydrogen disks whose rotational velocities increase beyond the optical disks, then $V_{max}(21)$ would be larger than V_{max} (opt). Observations of the required accuracy do not exist. Values of $V_{max}(21)$, accurate to $\pm 20\text{ km s}^{-1}$ on the plane of the sky, have been published for 11 of these galaxies (Paper IV; Shostak 1978), and unpublished values exist for three more. The mean difference,

$$\langle V_{max}(21) - V_{max}(\text{opt})\rangle = 0 \pm 4\text{ km s}^{-1},$$

and mean absolute difference

$$\langle |V_{max}(21) - V_{max}(\text{opt})|\rangle = +11 \pm 2\text{ km s}^{-1},$$

both independent of R. From this material, there is no evidence that the maximum rotational velocities differ from 21 cm and optical observations. More accurate velocities at both wavelengths will be necessary to place tighter constraints on the rotational velocities beyond the optical galaxy.

6. Rotational properties and morphology are related. Small galaxies are more likely to have ragged, filamentary arms; large galaxies are more likely to have global spiral patterns. This characteristic may be understood in terms of the differential properties of the rotation curves at small and large R. Angular velocity, V/R, is a more rapidly varying function of R at small R, so the differential effect is greatest here. V/R is a slowly varying function at large R, so the differential effects are minimized at large R. Preserving spiral structure is less of a problem for very large galaxies. This correlation helps to account for the success of the van den Bergh (1960) luminosity classification system, which identifies high luminosity (i.e., intrinsically large) spirals solely on the basis of their appearance. Statistically, intrinsically large spirals do tend to be more attractive than small ones. These considerations also support the use of linear diameter as a valuable tool for statistical studies.

7. From the normal emission line ratios at large nuclear distances, we infer that normal star formation is taking place at nuclear distances as great as 80 kpc. Additionally, the rotational properties of enormous galaxies like UGC 2885 can put constraints on models of galaxy formation and evolution. The outer parts of UGC 2885 have rotated fewer than 10 times in the age of the universe, but UGC 2885 is an attractive two-armed spiral with a regular velocity field. This regularity suggests that well-ordered global spiral patterns must be established soon after galaxy formation.

We thank the directors of Kitt Peak National Observatory, Cerro Tololo Inter-American Observatory, Lowell Observatory, and Hale Observatories for telescope time. We also thank Dr. P. J. E. Peebles for emphasizing the importance of very large galaxies, Dr. J. Kormendy for insight into the morphology questions, Drs. Seiden and Gerola for calculating computer analogs for each of these galaxies, Dr. A. Sandage for supplying the Revised Shapley Ames Catalogue in advance of publication, Dr. B. T. Lynds for information concerning the night sky wavelengths, Dr. J. Huchra for supplying galaxy velocities in advance of publication as a help in galaxy selection and Dr. D. Burstein for many conversations. We also thank Dr. Bruce Carney for taking the 4 m plates of NGC 801, 7664, and UGC 2885.

REFERENCES

Aaronson, M., Huchra, J., and Mould, J. 1979, *Ap. J.*, **229**, 1.
Bass, A. M., and Garvin, D. 1962, *J. Molec Spectrosc.*, **9**, 114.
Bertin, G., Lau, Y. Y., Lin, C. C., Mark, J. W.-K., and Sugiyama, L. 1977, *Proc. Nat. Acad. Sci.*, **74**, 4726.
Bosma, A. 1978, Ph.D. dissertation, Rijksuniversiteit te Groningen.
Burbidge, E. M., and Burbidge, G. R. 1964, *Ap. J.*, **140**, 1445.
Burns, J. O., and Owen, F. 1979, preprint.
Burstein, D. 1980, in preparation.
Burstein, D., and Heiles, C. 1979, unpublished.
de Vaucouleurs, G. 1975, in *Stars and Stellar Systems*, Vol. **9**, *Galaxies and the Universe*, ed. A. Sandage, M. Sandage, and J. Kristian (Chicago: University of Chicago Press), p. 557.
de Vaucouleurs, G., de Vaucouleurs, A., and Corwin, H. G. 1976, *Second Reference Catalogue of Bright Galaxies* (Austin: University of Texas Press) (RC 2).
Dressel, L. L., and Condon, J. J. 1978, *Ap. J. Suppl.*, **36**, 53.
Fisher, J. R., and Tully, R. B. 1977, *Comments Ap.*, **7**, 85.
Gerola, H., and Seiden, P. E. 1978, *Ap. J.*, **223**, 129.
Goad, G. W., De Veny, J. B., and Goad, L. E. 1979, *Ap. J. Suppl.*, **39**, 439.
Holmberg, E. 1958, *Medd. Lund. Astr. Obs.*, Ser. II, Nr. 136.
Kormendy, J., and Norman, C. A. 1979, *Ap. J.*, **233**, 539 (KN).
Kormendy, J., and Rubin, V. C. 1980, in preparation.
Kraan-Korteweg, R. C. and Tammann, G. A. 1979, preprint.
Krumm, N. and Salpeter, E. E. 1979, *A. J.*, **84**, 1138.
Lynds, B. T. 1979, private communication.
Nilson, P. 1973, *Uppsala General Catalogue of Galaxies* (*Uppsala Obs. Ann.*, Vol. **6**) (UGC).
Peterson, C. J., Rubin, V. C., Ford, W. K., Jr., and Roberts, M. S. 1978, *Ap. J.*, **226**, 770 (Paper III).
Peterson, C. J., Rubin, V. C., Ford, W. K., Jr., and Thonnard, N. 1976, *Ap. J.*, **208**, 662.
Roberts, M. S. 1978, *A. J.*, **83**, 1026.
Rubin, V. C., and Burstein, D. 1980, in preparation.
Rubin, V. C., Ford, W. K., Jr., Strom, K. M., Strom, S. E., and Romanishin, W. 1978, *Ap. J.*, **224**, 782 (Paper II).
Rubin, V. C., Ford, W. K., Jr., and Thonnard, N. 1978, *Ap. J. (Letters)*, **225**, L107 (Paper IV).
Rubin, V. C., Thonnard, N., and Ford, W. K., Jr. 1977*a*, *Ap. J. (Letters)*, **217**, L1 (Paper I).
———. 1977*b*, *Carnegie Yrb.*, **76**, 724.
Sandage, A., and Tammann, G. A. 1976, *Ap. J.*, **210**, 7.
———. 1980, *Carnegie Institution*, in press (RSA).
Sargent, W. L. W., Young, P. J., Boksenberg, A., Shortridge, L., Lynds, C. R., and Hartwick, F. D. A. 1978, *Ap. J.*, **221**, 731.
Searle, L. 1976, *R.O.B.*, **182**, 119.
Seiden, P. E., and Gerola, H. 1979, unpublished.
Shostak, G. S. 1978, *Astr. Ap.*, **68**, 321.
Sulentic, J. W. 1977, *Ap. J. (Letters)*, **211**, L59.
Thonnard, N., Rubin, V. C., Ford, W. K., Jr., and Roberts, M. S. 1978, *A.J.*, **83**, 1564.
Tully, R. B. 1974, *Ap. J. Suppl.*, **27**, 437.
Tully, R. B., and Fisher, J. R. 1977, *Astr. Ap.*, **54**, 661 (TF).
van den Bergh, S. 1960, *Ap. J.*, **131**, 215.
van der Kruit, P. D. 1973, *Ap. J.*, **186**, 807.
van der Kruit, P. C., and Bosma, A. 1978, *Astr. Ap. Suppl.*, **34**, 259.
Young, P. J, Westphal, J. A., Kristian, J., Wilson, C. P., and Landauer, F. P. 1978, *Ap. J.*, **221**, 721.
Zwicky, F., and Kowal, C. T. 1968, *Catalogue of Galaxies and Clusters of Galaxies*, Vol. **6** (Pasadena: Caltech), p. 244.

W. Kent Ford, Jr., Vera C. Rubin, Norbert Thonnard: Department of Terrestrial Magnetism, Carnegie Institution of Washington, 5241 Broad Branch Road, N.W., Washington, DC 20015

PLATE 17

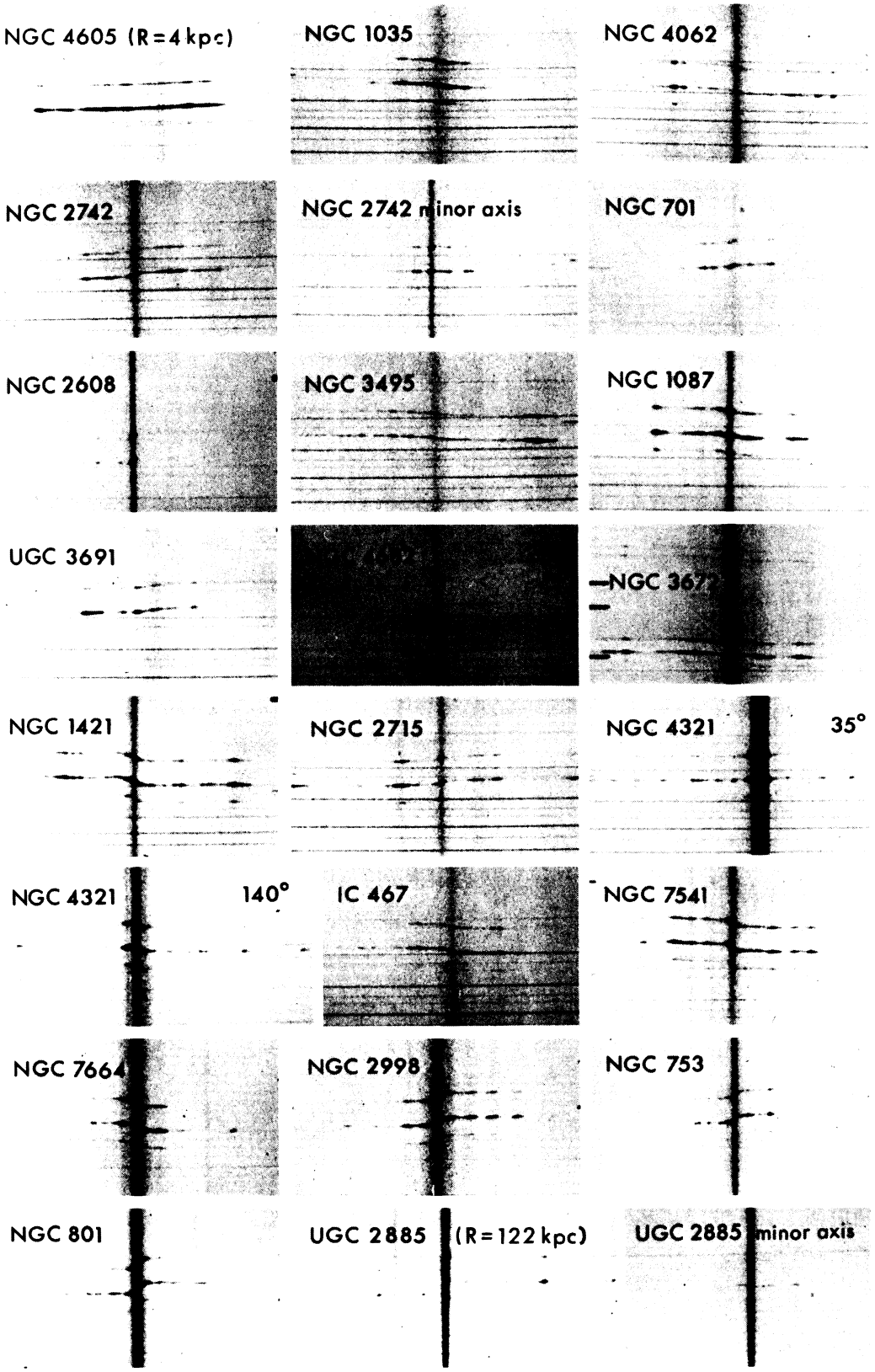

FIG. 1

RUBIN *et al.* (*see* page 474)

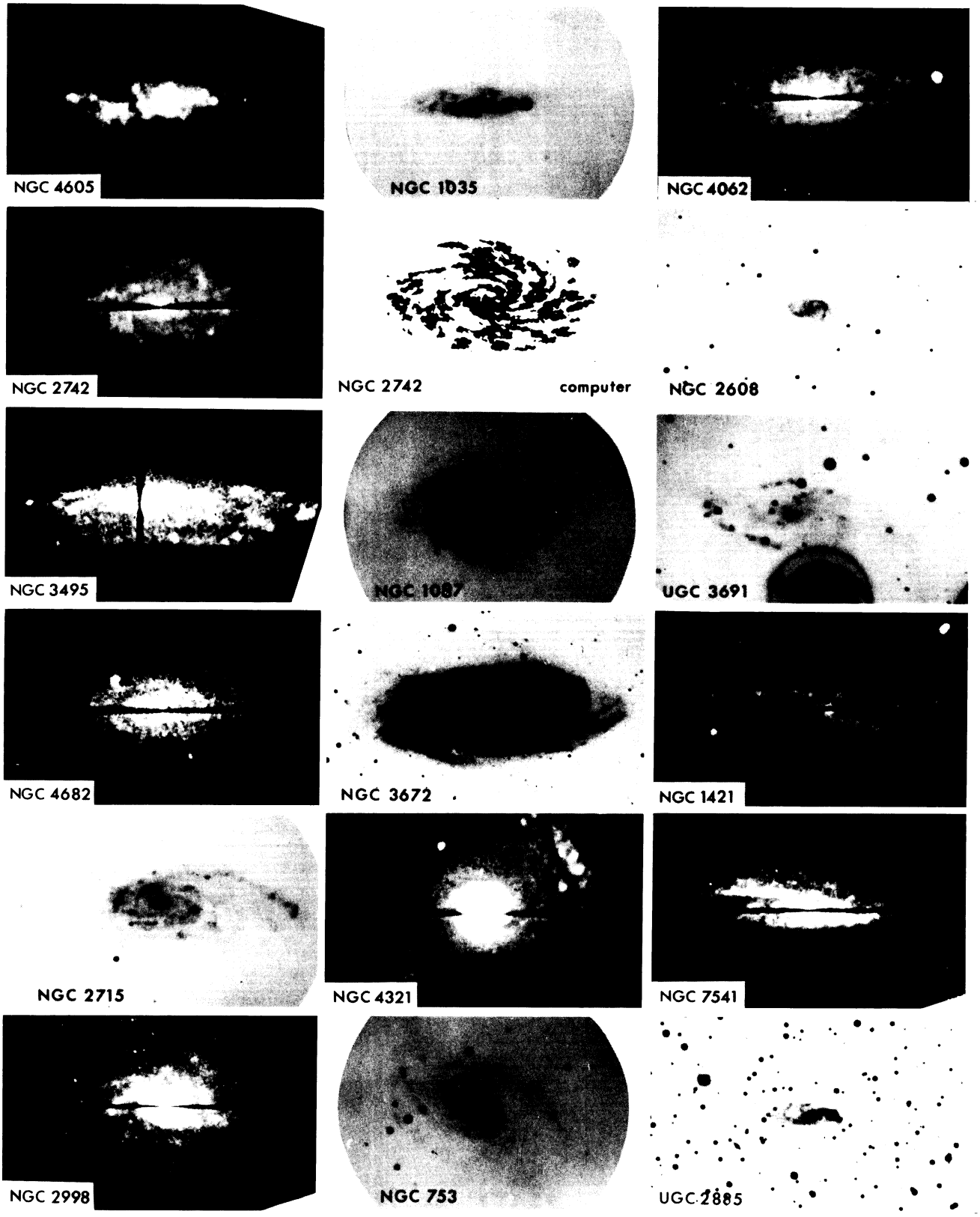

FIG. 2

RUBIN *et al.* (*see* page 474)

PLATE 19

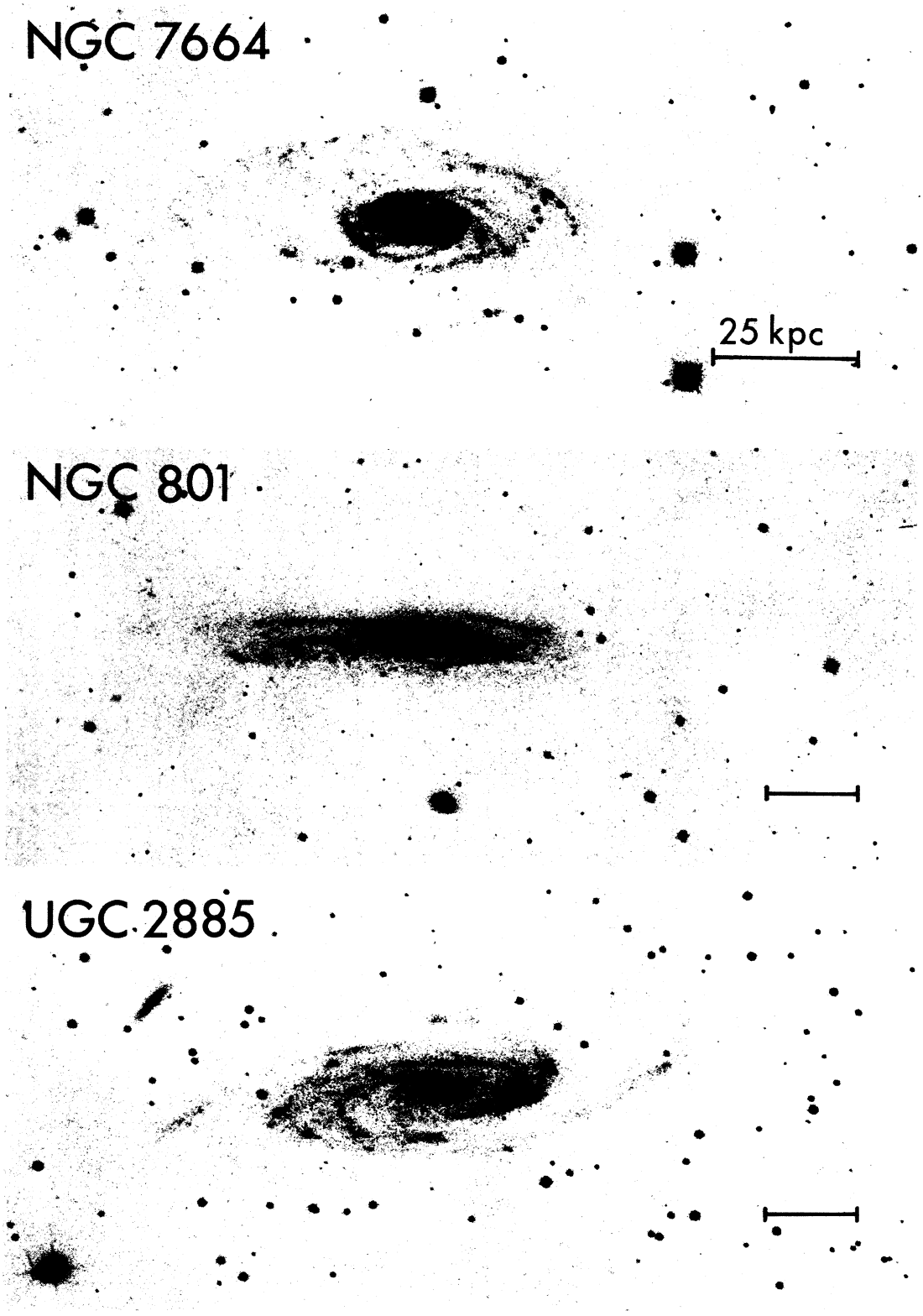

FIG. 3

RUBIN *et al.* (*see* page 474)